Polymer Bulletin (2019) 76:5577–5602
https://doi.org/10.1007/s00289-018-02670-2

ORIGINAL PAPER

Investigations on lithium acetate-doped PVA/PVP solid polymer blend electrolytes

K. Sundaramahalingam[1] · M. Muthuvinayagam[2] · N. Nallamuthu[2] · D. Vanitha[2] · M. Vahini[1]

Received: 13 September 2018 / Revised: 18 December 2018 / Accepted: 21 December 2018 /
Published online: 1 January 2019

Abstract

Lithium ion conducting solid polymer blend electrolytes (SPBE) are prepared using the host polymers poly[vinylalcohol] (PVA), poly[vinyl pyrrolidone] (PVP) and the lithium acetate. The complexation between the polymers and salt is confirmed by X-ray diffraction (XRD) and Fourier transform infrared spectroscopy (FTIR). The glass transition temperature of the prepared polymer electrolytes is determined by differential scanning calorimeter. Surface morphology of the polymer electrolytes is identified by scanning electron microscopy. Ionic conductivity of the solid electrolytes is studied using impedance analyzer in the frequency range of 42 Hz–1 MHz. The higher electrical conductivity of 5.79×10^{-6} S cm^{-1} and 1.400×10^{-4} S cm^{-1} is determined for 50PVA:50PVP:25 wt% lithium acetate system at 303 K and 363 K temperature, respectively. The dielectric and loss tangent analysis is also carried out for prepared polymer electrolyte and the higher-conductivity sample at different temperatures. The transference numbers of polymer electrolytes are calculated by Wagner's polarizing technique and also confirmed by Bruce–Vincent technique.

Keywords PVA/PVP · XRD · DSC · Ionic conductivity · Transference number

Introduction

In modern technology, polymers have been widely used due to the miniaturization of devices in various applications [1–5]. The electrical conductivity can be obtained by modifying the structure of the insulating polymer chain by doping of metallic ions [3]. The electrochemical properties of the polymers can also be improved by adding

✉ M. Muthuvinayagam
mmuthuvinayagam@gmail.com

[1] Multi-functional Materials laboratory, International Research Center, Kalasalingam Academy of Research and Education, Krishnankoil 626 126, India

[2] Department of Physics, School of Advanced Sciences, Kalasalingam Academy of Research and Education, Krishnankoil 626 126, India

different dopants [4–8]. In lithium batteries, the solid electrolyte is selected based on the best performance in operating temperature range, cell capacity, cyclic ability of the batteries and safety issues. In recent decades, enormous efforts have been made for the development of solid polymer electrolytes based on polyvinyl alcohol (PVA), polyvinylpyrrolidone (PVP), polyethylene glycol (PEG), polyacrylonitrile (PAN), polyethylene oxide (PEO) and polyvinylidene fluoride (PVdF). In 2015, Sandu et al. [9] reported PAN-co-PVAc/PVA-based bio-component polymer membrane for covalent immobilization of enzymes. Caprarescu et al. [10, 11] reported in 2017 about fruit extract (rosehip) mixed with PVA for treatment of crystal violet. Ebrasu et al. [12] and Caprarescu et al. [13] reported about the conducting polymer PAN doped with nanoparticle SiO_2 for fuel cell applications. In 2003, M.Z.A Yahya et al. reported that chitosan-based lithium acetate electrolyte shows lithium ion conductivity in the order of $\sim 10^{-5}$ S cm^{-1} using plasticizer [14]; moreover, to improve conductivity of polymer electrolyte, lithium acetate salt was mixed with PEO polymer matrix to show the conductivity in order of $\sim 10^{-6}$ S cm^{-1} [15].

Most of the industries use poly (vinyl alcohol) (PVA) as an effective polymeric matrix to achieve the desired properties. For an example, a solid polymer electrolyte was prepared by doping phosphoric acid with PVA; the resultant can be used as a electrolyte in solid-state electrochromic displays and solid-state photocells [16].

PVA is a semicrystalline polymer. It exhibits unique physical character consequent from crystal-amorphous interfacial effects [17, 18]. PVA is one of the biodegradable, nontoxic polymers [19–21]. It helps to improve electrochemical properties due to the presence of OH groups bonding between carbon chain backbone molecules. PVA-lithium acetate TiO_2 system shows better conductivity as 4.5×10^{-6} S cm^{-1} [22, 23]. To attain desirable electrochemical properties and higher conductivity, polymer blending is necessary for developing electrochemical devices.

Polyvinylpyrrolidone (PVP) polymer is conjugated polymer and also has excellent properties such as complex-forming abilities, high environmental stability, easy process ability, thermal conductivity and water absorption [24, 25]. Jaipal Reddy et al. [26, 27] fabricated thin-film electrochemical cell by developing PVP + $AgNO_3$ and PVP + $NaNO_3$ as solid electrolyte. Solid electrolyte is a material with viscoelastic properties that can accommodate for the volume change during the ion–electron exchange process, and such mechanical property needs a disordered structure, a feature favorable to ionic conductivity [28]. The influence of PVP on the crystallinity of PVA and optical band gap of the blend has been studied by Zidan et al. [29]. By their reports, it is confirmed that the crystallinity of PVA decreases with increasing the level of PVP. PVA/PVP blends are suitable to film formation with higher disorder and miscible in all ratios, due to hydroxyl group of PVA and carbonyl group of PVP. PVP is focusing for its hydrophobicizer and mechanical properties [21, 30].

The choice of polymer electrolytes in modern applications, such as high energy density batteries, electrochromic devices, dye-sensitized solar cells, supercapacitors, electric vehicles, sensors and actuators, and fuel cells, was justified by studying their structural, morphological and electrical properties.

In this manuscript, the composition of 50PVA/50PVP has been selected for their stability and also the particular composition has the highest conductivity value than the other compositions. From the earlier reports, the maximum conductivity has

been found to be 10^{-8} S cm^{-1} at room temperature for 50PVA:50PVP polymer blend electrolyte with water as a solvent [31].

Li-ion battery has become the primary one for the next-generation power production. Li-ion batteries offer the largest energy density and output voltage. Lithium acetate is one of the low-cost lithium salts than others and has high solubility in most of the solvents [15], so that blend polymer electrolytes based on PVA/PVP/lithium acetate were prepared to improve the ionic conductivity.

Materials and methods

PVA 50 wt%, PVP 50 wt% and *x* wt% of lithium acetate ($x = 5$, 10, 15, 20, 25 and 30) of indifferent compositions were prepared. The precursor materials had been taken such as analytical grade poly (vinyl alcohol) (PVA) mw = 14,000 g/mol, poly (vinyl pyrrolidone) (PVP) mw = 90,000 g/mol which were purchased from SD Fine Chem Ltd., India. Lithium acetate with mw = 102.02 g/mol was also purchased from Merck, India, to prepare blend polymer film. The precursor PVA was added with distilled water to obtain the clear transparent solution. Likewise, PVP and lithium acetate solutions were also prepared separately. Those prepared solutions were mixed together and stirred well for 24 h to get the homogeneous solution. The final solution was then poured into polypropylene dishes and dried at ambient temperature to confirm the removal of excess solvent traces. The flexible uniform and transparent films had been obtained and retained in the desiccators for further characterization. Figure 1a shows the preparation method of blend polymer electrolyte, and Fig. 1b shows the photograph of film.

The prepared blend polymer films were characterized by several techniques. The XRD pattern of the blend polymer electrolyte was recorded using Bruker make X-Ray diffractometer having CuKα radiation ($\lambda = 1.540$ Aº) with scanning rate 5° per minute in the range of 10°–80°. FTIR Transmittance spectra of the films were recorded using "SHIMADZU IR Tracer 100" Spectrometer with a resolution of 4 cm^{-1} and the wave number range of 400–4000 cm^{-1}. The prepared electrolytes were characterized by PerkinElmer 4000 Differential Scanning calorimeter in the temperature range between 50 and 400 °C at the scanning rate of 10 °C min^{-1}. The Carl ZEISS EVO 18 scanning electron microscope was used to study the surface morphology of the polymer electrolytes. The impedance measurements were done by the computer-controlled HIOKI 3532-50 LCR Hi-tester in the frequency range of 42 Hz–1 MHz for the temperature range of 303–363 K.

Result and discussion

XRD analysis

The structural studies of lithium acetate mixed with 50 wt% PVA:50 wt% PVP blend were performed using XRD pattern, and the recorded pattern is shown in Fig. 2. PVA is semicrystalline in nature. In the XRD spectrum of PVA, the sharp peaks

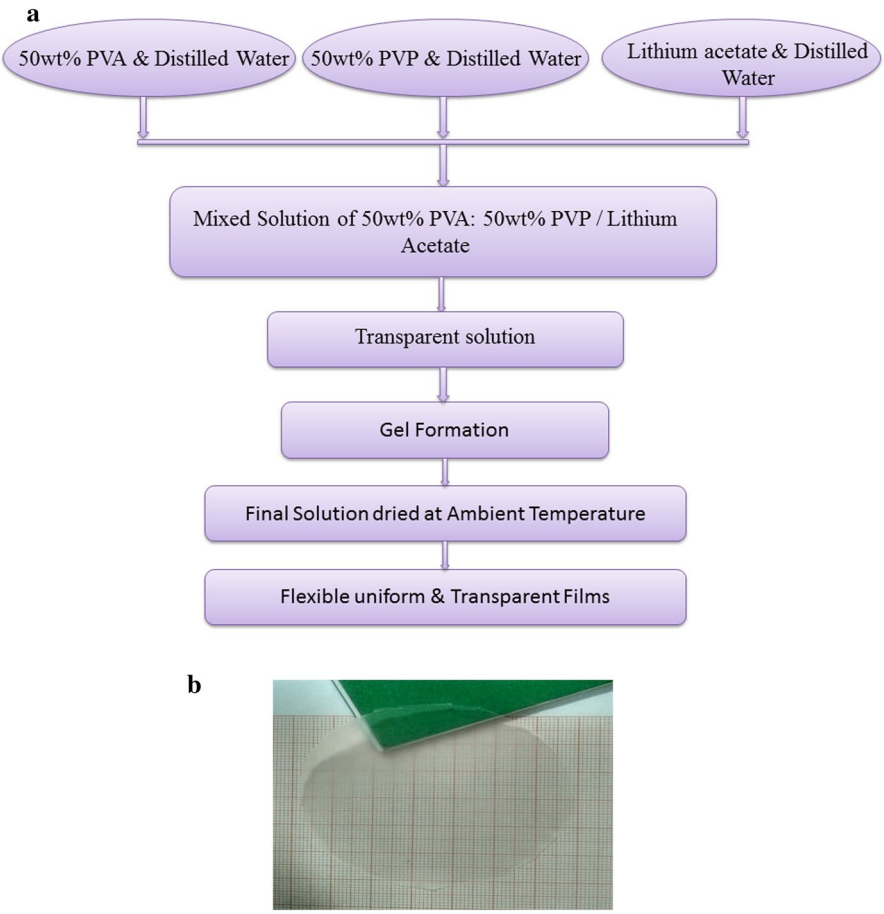

Fig. 1 **a** Preparation of PVA/PVP/lithium acetate blend polymer electrolytes. **b** Photograph of prepared transparent solid polymer electrolyte

appeared at $2\theta = 20°$, 40° are reported [32] in Fig. 2. The peak appeared at $2\theta = 40°$ vanishes for pure PVA/PVP blend polymer. The small broadened hump appeared at $2\theta = 20°$ which indicates the increase in amorphous nature of the PVA in blend polymer. In higher composition, the hump at $2\theta = 31°$ and 40° appeared due to the inclusion of LiAce in polymer matrices. This is mainly due to the short range order of LiAce in PVA/PVP blend polymer matrix [33]. By increasing the concentration of LiAce, the broadness of the hump is decreased which indicates the increasing amorphous nature in the compositions. The interactions between functional groups of PVA, PVP and dopant ions (Li^+ and CH_3COO^-) result in the displacement of ions from their lattice sites. The displacement created the dislocations; thereby, the broadening of the diffracted x-ray hump is observed. This indicates the increase in the amorphous nature of the host polymer with the increase in lithium acetate concentration [34].

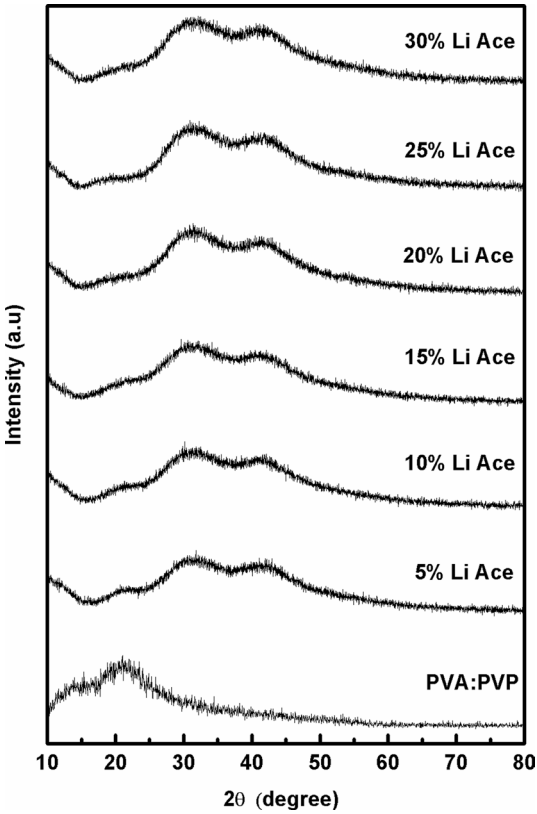

Fig. 2 XRD patterns of 50 wt% PVA:50 wt% PVP blends with different concentrations of lithium acetate

FTIR analysis

The bond formation in polymer electrolyte is investigated by FTIR spectroscopy. It provides information of interactions between various constituents and the complexation in the polymer sample. The IR spectra of different concentrations of lithium acetate blend with 50 wt% PVA:50 wt% PVP electrolytes are shown in Fig. 3.

For pure PVP, band observed at about 1564 cm^{-1} is allotted to the characteristic vibration of C=N (pyridine ring). The transmission band at 928 cm^{-1} is assigned to the out-of-plane rings of C=H bending [35].

On the other hand, for pure PVA, the wide transmission band at about 3340 cm^{-1} is attributed to O=H stretching vibration of hydroxyl group [35]. The IR bands of the polymer blend 50 wt% PVA:50 wt% PVP:lithium acetate at 3340, 2931, 1640, 1417, 1019 and 928 cm^{-1} are attributed to the O–H stretching, CH_2 asymmetric stretching, C=O stretching, CH_2 bending, C–O stretching and C–O Symmetric stretching, respectively, which have been observed as syndiotacticity of PVA [36]. The band is shifted due the interaction between the hydroxyl group of PVA and carbonyl group of PVP with the addition of LiAce. The band at about

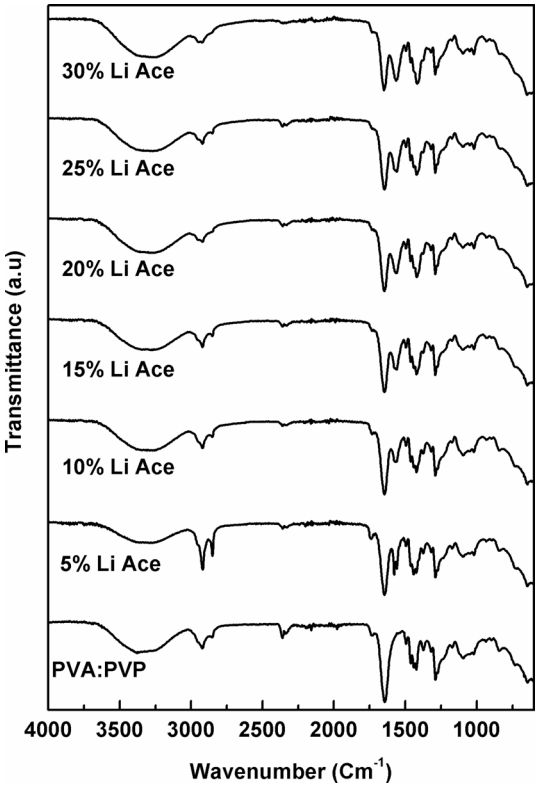

Fig. 3 FTIR spectra of 50 wt% PVA:50 wt% PVP blend with different concentrations of lithium acetate

1271 cm^{-1} corresponds to C=O stretching of acetyl groups present on the PVA backbone. While increasing the concentration of LiAce, the intensity of the band decreased, indicating the transition from the semicrystalline nature to amorphous as indicated in XRD. The vibrational band at about 1647 cm^{-1} corresponds to C–O symmetric bending of PVA and PVP [37, 38].

While blending PVA/PVP with different concentrations, lithium acetate results in the shifting of peaks position, shape and intensity and it is tabulated in Table 1.

The shift in stretching modes of the carbonyl bonds due to pyrrolidone rings is realized from peaks in the region 1640–1649 cm^{-1}. The various vibrational frequencies and their assignments are given in Table 1. It is noticed that the peak at 2843 cm^{-1} disappears for 30 wt% lithium acetate blend polymer electrolyte. The peak at 1640 cm^{-1} is decreasing when increasing lithium acetate salt concentration to PVA/PVP polymer electrolyte. The detected shifts and deviation in intensities of the FTIR spectrum of the blend suggest the complete complexation of salt with polymer blend [36].

DSC analysis

Thermal properties of the polymer electrolytes can be predicted by using the differential scanning calorimetry (DSC). The DSC curves for pure PVA/PVP blend and

Table 1 Vibrational frequencies of PVA/PVP/lithium acetate system

Assignment	Wavenumber (cm^{-1})						
	PVA/PVP	5% Li Ace	10% Li Ace	15% Li Ace	20% Li Ace	25% Li Ace	30% Li Ace
O–H stretching	3340	3329	3314	3316	3311	3318	3304
CH_2 asymmetric stretching	2931	2920	2921	2921	2920	2921	2921
C–H stretching	2843	2849	2849	2848	2851	2848	2850
CH_2 bending	1417	1413	1419	1418	1419	1420	1418
C–O stretching	1019	1013	1021	1017	1015	1017	1018
C=O stretching	1640	1645	1648	1645	1649	1643	1648
C–N stretching	1564	1579	1569	1579	1564	1558	1562
C–O symmetric stretching	928	932	934	930	930	932	932

PVA/PVP with different compositions of lithium acetate are given in the figure in the range of 30–400 °C. In all the DSC thermograms, a step change between 120 and 140 °C denotes the glass transition temperature of the polymer electrolytes. The endothermic peaks appeared in the figure relating the melting temperature (T_m) of polymer electrolytes. This arises due to the melting of crystalline phase of polymer PVA. The values of T_g, T_m enthalpy and the degree of crystallization are given in Table 2.

The glass transition of the polymer electrolytes decreases by increasing the salt concentration as shown in Fig. 4. This indicates the plasticization of the electrolytes by increasing the salt concentration and also enhancing the amorphous nature of the blend polymer electrolytes. The dipole–dipole interaction between the PVA and PVP chains is weakened due to the addition of the salt with the polymer blend. All the polymer blend electrolytes are having single glass transition temperature. This indicates the miscibility of the polymer electrolytes.

For higher-conductivity polymer electrolyte, there exists a low glass transition temperature. The higher conductivity arises due to the higher segmental motion of the polymer electrolyte. The segmental motion produces free volume that enables the free flow of ions through the polymer chain network under applied electric field. The degree of crystallinity can be calculated through the enthalpy of the melting point endothermic curve T_m. It is the ratio of melting heat (ΔH_m) of polymer electrolytes to the melting heat (ΔH_0) for 100% crystalline PVA phase by the following relation:

$$X_c = \left(\Delta H_m / \Delta H_0\right) \times 100 \tag{1}$$

The degree of crystallinity of the polymer electrolytes decreases by increasing the salt concentration.

SEM analysis

The compatibility between dissimilar components through the perception of phase separations and interfaces can be found by using scanning electron microscope

Table 2 Enthalpy and degree of crystallinity of 50PVA:50PVP with different concentrations of lithium acetate

Composition	T_g in degree	Enthalpy	Degree of crystallinty (%)
50PVA:50PVP	141	90.78	64
50PVA:50PVP:5 wt% lithium acetate	115	81.46	58.8
50PVA:50PVP:10 wt% lithium acetate	112	57.24	41.3
50PVA:50PVP:15 wt% lithium acetate	108	49.08	35
50PVA:50PVP:20 wt% lithium acetate	100	26.6	33
50PVA:50PVP:25 wt% lithium acetate	97	46.0186	26.6
50PVA:50PVP:30 wt% lithium acetate	109	82.0203	59.17

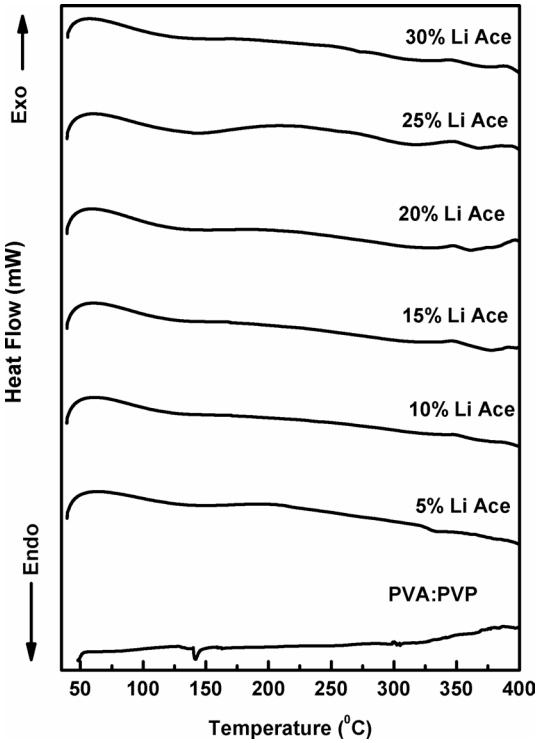

Fig. 4 DSC thermograph of various compositions of lithium acetate-doped PVA/PVP polymer electrolytes

(SEM). The surface morphology of different concentrations of lithium acetate blend with PVA/PVP polymer electrolyte is in the magnification of 5000 times and range 2 µm as shown in Fig. 5a–f. SEM images show the variation of the distribution of lithium acetate in blend polymer films. In Fig. 5a–f, the smooth surface indicates the uniform distribution and also the complex dissolution of salt in the blend polymer film. At higher concentration of 30 wt% of lithium acetate, some crystallites are observed in blend polymers. Even though XRD results show amorphous nature, it may be formed by less dissolution of salt in the blend polymer matrix.

Ac impedance analysis

Cole–cole plot

Ac impedance technique is the best tool to study the electrical properties of the polymer electrolyte. The cole–cole plots for 50 wt% PVA/50 wt% PVP with various concentrations of lithium acetate are shown at room temperature in Fig. 6. For 5 wt% lithium acetate, there exists a semicircle which is equivalent to the parallel combination of bulk resistance and bulk capacitance [39, 40]. For 10 wt% lithium acetate, a semicircle with a spike occurred. The equivalent circuit is the series capacitance with parallel combination of resistance and capacitance. Furthermore,

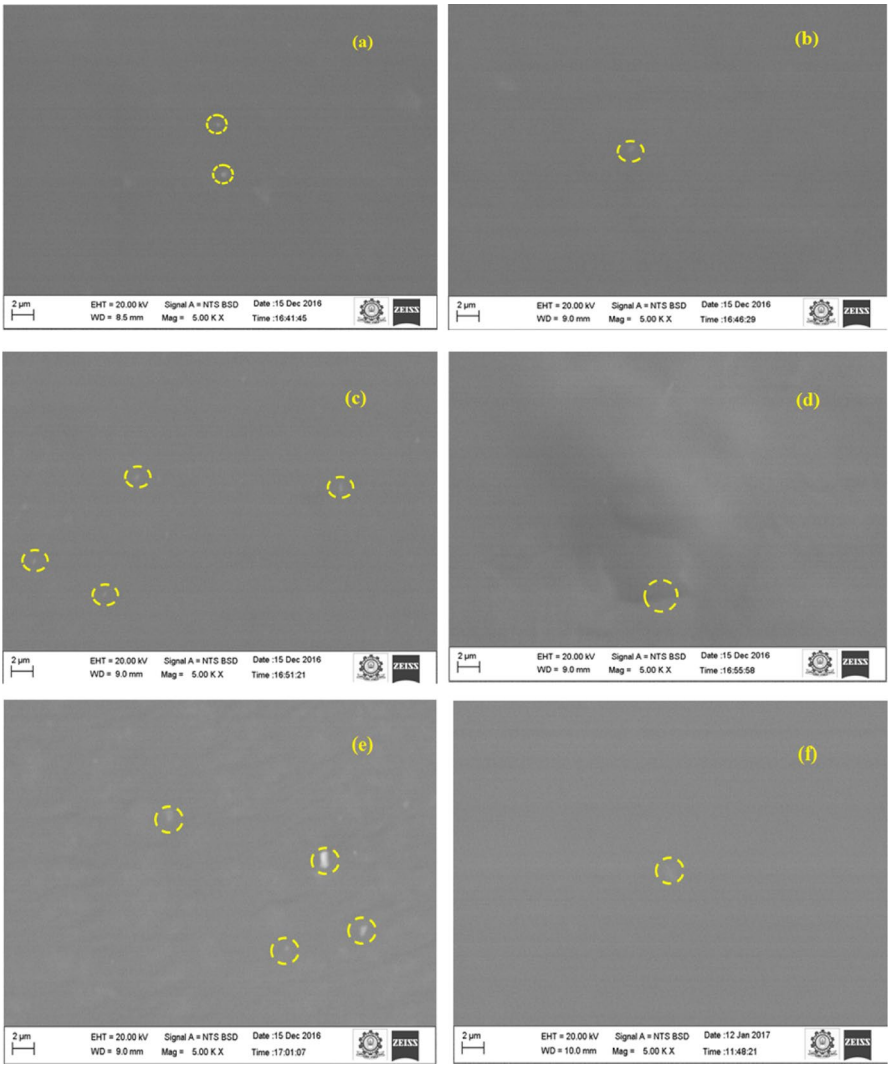

Fig. 5 **a–f** SEM images of 50 wt% PVA:50 wt% PVP with 5–30 wt% concentrations of lithium acetate

for the other compositions (15–30 wt% lithium acetate), the impedance plot shows two semicircles with a spike. In cole–cole plot, the first semicircle is formed as non-Debye behavior which is due to the indication of ion relaxation in amorphous nature of polymer matrices. The second semicircle is also formed as non-Debye behavior which is mainly due to the ion relaxation in short range order of LiAce-incorporated polymer matrices [41]. The equivalent circuit is shown in Fig. 7.

The total resistance is measured by the extension of spike which touches on the x-axis in the cole–cole plot. The total resistance can be calculated by fitting of the impedance using the Z view software.

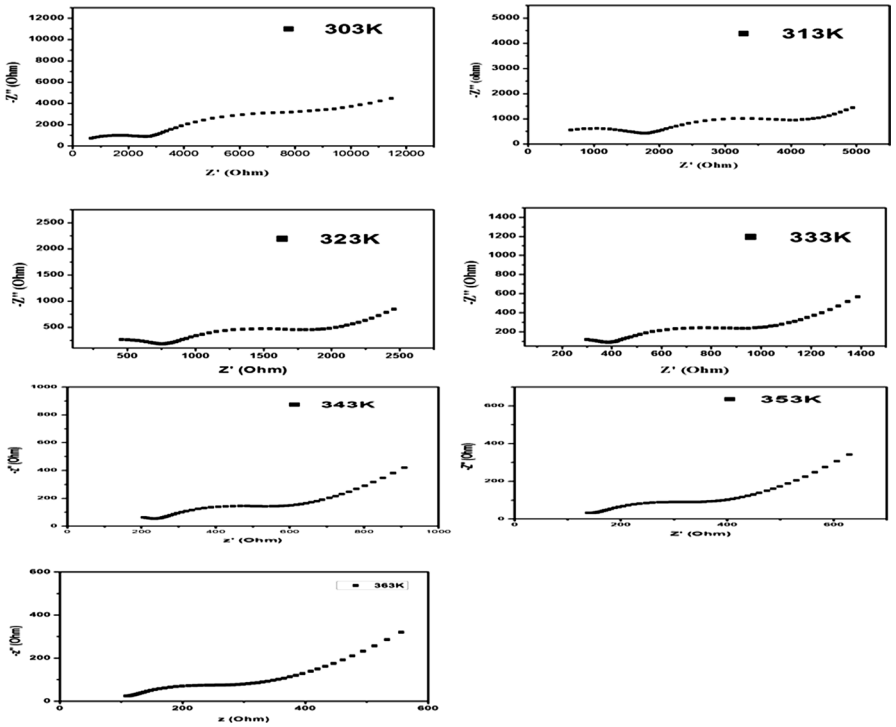

Fig. 6 Cole–cole plot for 50 wt% PVA:50 wt% PVP blend with 25 wt% of lithium acetate at different temperatures

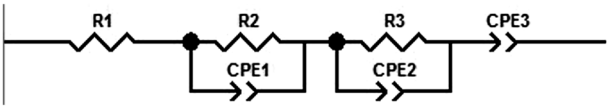

Fig. 7 Equivalent circuit of polymer electrolyte

The bulk conductivity is calculated using the formula,

$$\sigma = l/RA \tag{2}$$

where l and A are the thickness and area of the electrolyte, respectively, and R is the total resistance of the electrolyte. The total conductivity of all compositions is calculated for the temperature range of 303–343 K. Figure 8a shows $1000/T$ versus log σT plot for all the blend polymer electrolytes, which obey the Arrhenius behavior. The activation energy (E_a) can be calculated using the slope of the following equation

$$\sigma T = \left(\sigma_0\right) \exp\left(-E_a/kT\right) \tag{3}$$

where σ_0 is the pre-exponential factor, E_a the activation energy, k Boltzmann constant and T Temperature. The electrical conductivity at ambient temperature and activation energy values are tabulated in Table 3 for all the compositions of blend

Fig. 8 **a** Temperature dependence of ionic conductivity of 50 wt% PVA:50 wt% PVP polymer blend electrolytes with different compositions of lithium acetate. **b** VTF plot of 50 wt% PVA:50 wt% PVP polymer electrolyte with 25 wt% of lithium acetate. **c** Temperature dependence of DC conductivity (modified Arrhenius equation) for 25 wt% lithium acetate-doped PVA/PVP polymer blend electrolyte ▶

polymer electrolyte. The activation energy decreases with increasing salt concentration leading to the enhancement of electrical conductivity with 25 wt% lithium acetate of blend polymer. This 25 wt% of lithium acetate blend that exhibits the maximum ionic conductivity possesses the activation energy values of 0.41 eV and 0.67 eV at higher and lower temperature regions, respectively. Lithium-based PVA/PVP polymer electrolytes have been given more attention to develop lithium-ion batteries. Rajeswari et al. [35] have already reported the higher conductivity for 70 PVA:30 PVP:25 Mwt% of $LiNO_3$ and 70 PVA:30 PVP:25 Mwt% of $LiClO_4$ is in the order of 10^{-4} S cm^{-1}. Deshmukh et al. [42] also reported the high ionic conductivity (1.15×10^{-5} S cm^{-1}) for the combination of 50PVA/50PVP/20 Li_2Co_3. In this paper, the higher electrical conductivity of 5.79×10^{-6} S cm^{-1} and 1.40×10^{-4} S cm^{-1} is determined for 50PVA:50PVP:25 wt% lithium acetate system at 303 K and 363 K, respectively. As compared to the earlier reports, the conductivity is improved for the prepared sample at high temperature. Rather at 30 wt% concentration, the activation energy increases and electrical conductivity decreases, and this may be due to the creation of blockages of charge carriers in conducting pathway due to the increased salt concentration.

Figure 9 represents the variation of activation energy for different weight percentages of lithium acetate concentration at different temperatures. The Vogel–Tamman–Fulcher (VTF) plot is the evidence of polymer segmental motions, and also nonlinear behavior of Arrhenius plot can be explained. Figure 8b shows the VTF plot of the high conductivity blend polymer electrolyte. The following equation explicated Vogel–Tamman–Fulcher (VTF)

$$\sigma = AT^{-1/2}\exp\left[\frac{-B}{k\left(T-T_0\right)}\right] \tag{4}$$

where A is the fitting constant, B pseudo-activation energy associated with the motion of the polymer segment and T_0 equilibrium temperature of the system corresponding at zero configuration entropy ($T_0 = T_g - 50$ K). The linear behavior in VTF plot shows the polymer segmental motion rather than hopping of ions [43].

The transport of ions through polymer matrix depends on the concentration of the salt and the dielectric constant [44]. The reformulated Arrhenius behavior is studied by using Aziz et al. [45–47]. Figure 8c denotes the variation of dc conductivity with respect to function of ($1000/\varepsilon'\times T$). The reformulated Arrhenius equation is given by the equation.

$$\sigma = \sigma_0 \exp(E_a / KT\varepsilon') \tag{5}$$

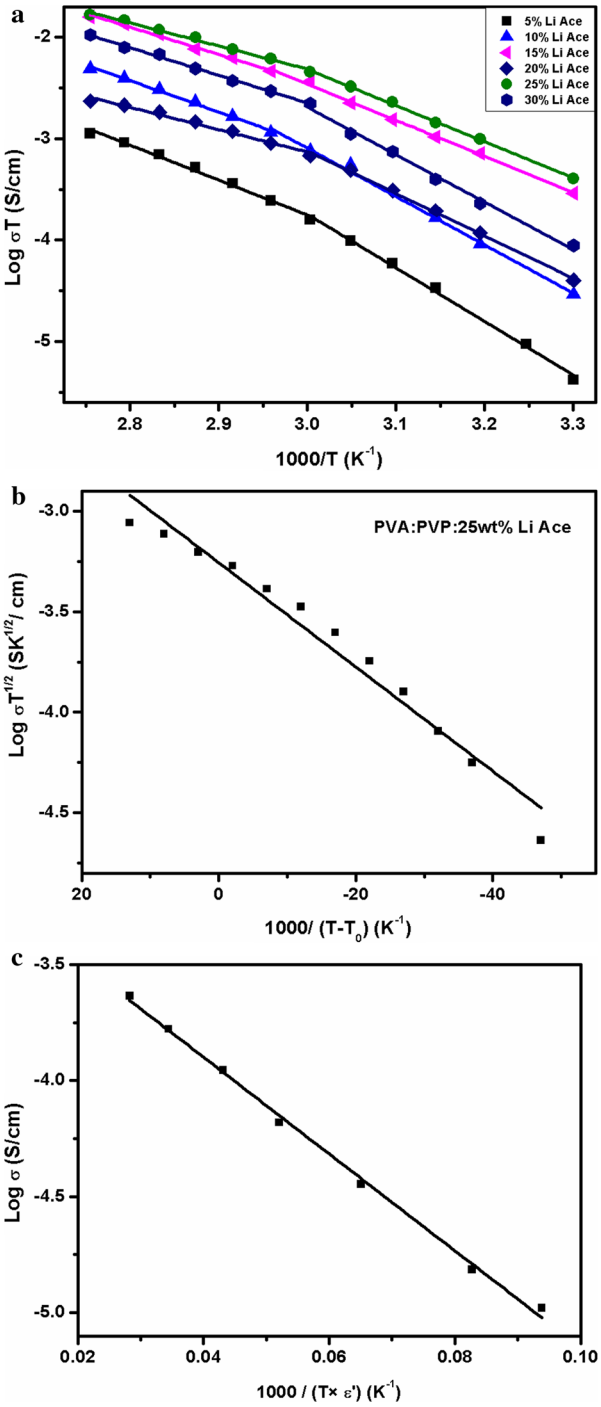
a
5% Li Ace
10% Li Ace
15% Li Ace
20% Li Ace
25% Li Ace
30% Li Ace
Log σT (S/cm)
1000/T (K-1)
b
PVA:PVP:25wt% Li Ace
Log σT1/2 (SK1/2/ cm)
1000/ (T-T0) (K-1)
c
Log σ (S/cm)
1000 / (T× ε') (K-1)

Table 3 Conductivity and activation energy of the 50PVA:50PVP blend with different weight percentages of lithium acetate

Composition	σ from cole–cole plot (S cm^{-1})	Activation energy (eV) at higher temperature region	Activation energy (eV) at lower temperature region
50PVA:50PVP:5 wt% lithium acetate	1.38×10^{-08}	0.65	1.00
50PVA:50PVP:10 wt% lithium acetate	2.31×10^{-07}	0.59	0.91
50PVA:50PVP:15 wt% lithium Acetate	6.7×10^{-07}	0.43	0.68
50PVA:50PVP:20 wt% lithium acetate	1.32×10^{-07}	0.51	0.80
50PVA:50PVP:25 wt% lithium acetate	5.79×10^{-06}	0.42	0.68
50PVA:50PVP:30 wt% lithium acetate	2.91×10^{-07}	0.51	0.89

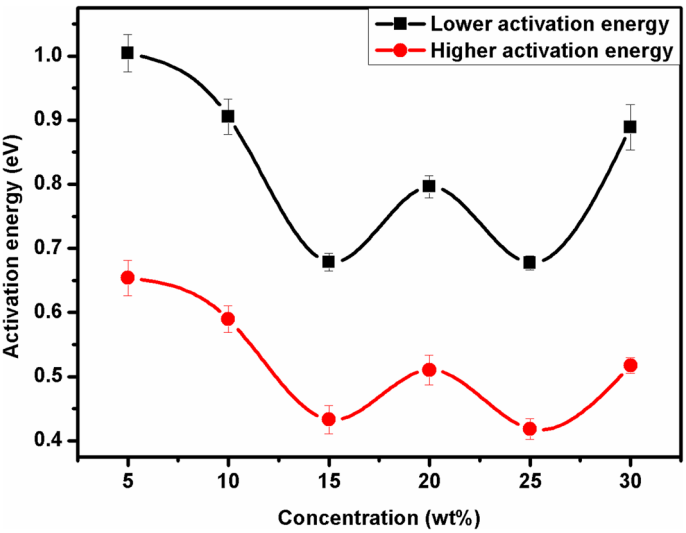

Fig. 9 Variation of activation energy for different wt% of lithium acetate concentrations

The linear straight line with a regression value of 0.99 is obtained from the graph. From this, it is concluded that the ion transport is related due to the dielectric constant.

Frequency-dependent electrical conductivity spectra analysis

The electrical conductivity (σ) as a function of angular frequency (ω) in the logarithmic plot for all the polymer blend electrolytes at room temperature is shown in

Fig. 10. As seen from Fig. 10, the frequency-dependent conductivity plots show six distinct regions. The first low-frequency dispersion region observed can be ascribed to the space charge polarization. The second and fifth regions are plateau region which is mentioned for dc conductivity. The third and fourth regions which are meant for dispersive regions are overlapped. The final dispersion region is formed due to oscillating charges at higher frequencies. Here, the two overlapped conductance spectra are observed.

Each frequency-dependent conductivity spectrum is analyzed using Jonscher power law [48].

$$\sigma(\omega) = \sigma_{dc} + A\omega^{n} \tag{6}$$

where A and n are temperature-dependent and σ_{dc} is dc conductivity. The dc conductivity and other parameters can be computed by fitting the experimental information with Jonscher power-law condition and are tabulated in Table 4. In the high-frequency region, the conductivity increases with the frequency. The mobility of charge carriers is higher in the high-frequency region [39].

Dielectric analysis

In order to study about the ion conduction, dielectric constant and dielectric loss are the important parameters. The ability of the polymer to dissolve salts is determined by dielectric constant. High dielectric constant reduces ion–ion interactions and also inhibits crystal formation. Figure 11a, b denotes the variation of dielectric constant and dielectric loss as a function of frequency for 50 wt% PVA:50 wt% PVP:25 wt% lithium acetate polymer blend electrolyte. From Fig. 11a, b, it is confirmed that

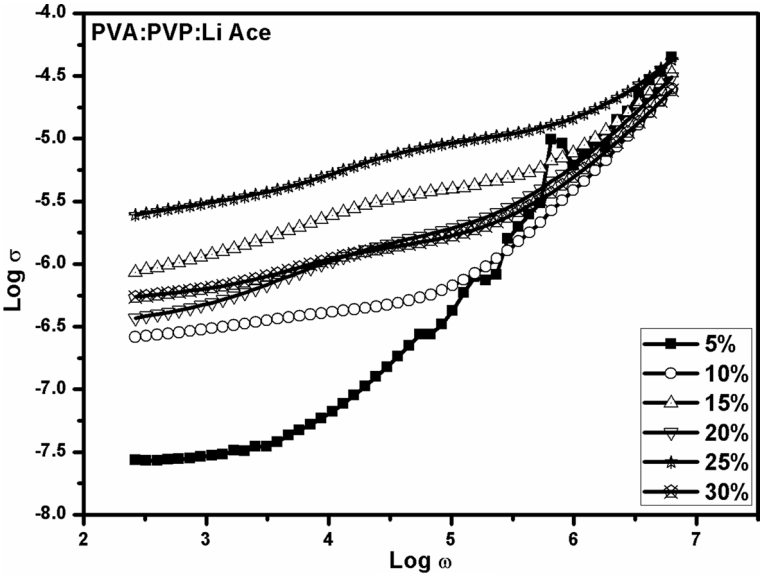

Fig. 10 Conductance spectra for 50 wt% PVA:50 wt% PVP blend with different wt% of lithium acetate

Table 4 Conductivity and temperature dependant constant values for 50PVA:50PVP:25 wt% lithium acetate blend polymer electrolyte with different temperatures

Temperature	$\sigma_{dc\ (high\ temperature\ region)}$	A_1	n_1	$\sigma_{dc\ (low\ temperature\ region)}$	A_2	n_2
303 K	9.35×10^{-6}	5.05×10^{-12}	0.99	1.72×10^{-6}	8.87×10^{-8}	0.39
313 K	1.49×10^{-5}	2.54×10^{-12}	0.98	4.91×10^{-6}	6.21×10^{-8}	0.45
323 K	3.43×10^{-5}	5.02×10^{-12}	0.95	1.04×10^{-5}	1.15×10^{-7}	0.45
333 K	6.41×10^{-5}	1.05×10^{-10}	0.80	1.08×10^{-5}	1.22×10^{-6}	0.30
343 K	8.75×10^{-5}	1.60×10^{-8}	0.42	2.53×10^{-5}	1.03×10^{-6}	0.33
353 K	9.75×10^{-5}	3.31×10^{-5}	0.11	3.76×10^{-5}	2.01×10^{-6}	0.30
363 K	1.40×10^{-4}	7.69×10^{-6}	0.16	5.86×10^{-5}	8.49×10^{-7}	0.38

there is an increase in ε´ with temperature. For all temperatures, there is a strong frequency dispersion of permittivity in the lower-frequency region, whereas at higher-frequency region, there is nearly frequency-independent behavior. This may be attributed to the electrical relaxation processes. In the low-frequency region, there exists a sharp increase in the dielectric constant with frequency indicating the presence of space charge polarization. As the temperature increases, the kinetic energy and thermal energy increase, thereby stimulating the movement of ions. The electrolyte behaves like a polar material that enables the dipole orientation [27] and increases the mobility of charge carriers. The addition of lithium acetate with the polymer blend may result from the localization of charge carriers along with mobile ions, thereby causing higher ion conductivity.

The same trend can be observed for the dielectric loss of the polymer system. The increase in the dielectric loss at low-frequency region may be due to the free ion movement within the materials. In addition to dopant material within the polymer blend, the dielectric loss increases in the lower-frequency region. The increase in the dielectric loss by increasing temperature is owing to the hopping of the charge carriers.

From Fig. 11c, it is confirmed that the dielectric constant increases by increasing the temperature for the higher-conductivity polymer electrolyte. The dielectric constant arises due to the separation of ions and the vibration of the polymer chain segment and thereby increasing the conductivity [49–51].

Concentration-dependent dielectric analysis

Dielectric constant for different compositions of polymer electrolytes over various frequencies at room temperature is depicted in Fig. 12a. From the figure, it is observed that the dielectric constant has been decreased exponentially with frequency and exhibits a frequency-independent behavior at high frequencies. The dielectric constant attained a maximum value for higher-conductivity polymer electrolyte. The maximum value may be due to the increase in the Li-ion conduction-related polarization. The maximum dielectric constant reduces ion–ion interactions and also prevents crystal formation [52, 53]. Figure 12b is used to find the dielectric constant from dielectric spectra.

Loss tangent analysis

Loss tangent or dielectric loss factor is the frequency-dependent parameter, which represents the energy dissipation in dielectric to analyze the electrical properties of polymers. Figure 13a shows the loss tangent spectra of 50 wt% PVA:50 wt% PVP:25 wt% lithium acetate at various temperatures. In Fig. 13b, there are two humps, which represent the formation of two relaxation times in non-Debye behavior. The loss tangent curve shifts toward higher frequencies with increasing temperatures [54]. The relaxation times τ_1 and τ_2 are observed from the peak frequencies in tan δ plots. Thus, the low frequency peaks are known as α relaxation peaks to the dynamic dipole rotation, and the high frequency peaks are known as β relaxation behavior due to dipole orientation in static region. It is illustrated in the loss tangent for various frequencies as shown in Fig. 13 a. From Fig. 13a, the β relaxation peak is large in 25 wt% of LiAce and it shifted toward higher frequencies which are related to possibility of ion relaxation in amorphous phase. These results are clearly in agreement with the structural XRD and impedance analysis. The loss tangent spectra of higher-conductivity polymer electrolyte with different temperatures are shown in Fig. 13b. In this, the high frequency peak is related to β relaxation of amorphous phase, whereas lower frequency peak is related to α relaxation of short range order. The height of tan δ peak value is decreased with the increase in the temperature, which may due to ion movement and creation of ions in the short range ordered polymer matrices. This is very well matched with the concept of temperature-dependent conductivity [55, 56].

Relaxation time as a function of temperature is plotted, and also the activation energy is calculated from the following formula,

$$\tau = \left(\tau_0\right) \exp\left(E_a/kT\right) \tag{7}$$

Activation energy is found to be 0.47 eV and 0.58 eV at lower and higher frequency due to relaxation time τ_1 and τ_2, respectively. It is consistent with impedance analysis results. Two different relaxation times are observed which is confirmed by impedance, conductance and loss tangent results.

Transference studies

Wagner's polarization technique Transference number is used to study the ion transport behavior in the polymer samples by Wagner's polarization technique. The ion transference number is calculated by Wagner's polarization technique. The prepared electrolyte is sandwiched between the two one-side graphite-coated silver electrodes. It is polarized by a constant dc potential of 1.5 V at ambient temperature [57]. There is an initial polarization current on the application of the potential, which is directly proportional to the applied field. When the electrical circuit is closed, the initial current identifies both electronic and ionic conductivity of the sample (i_t). And the final current is stable value due to the observed electronic current (i_e). The ionic transference number of the electrolyte can be calculated by the following equation.

$$t_{\text{ion}} = \left(i_t - i_e\right)/i_t \tag{8}$$

Fig. 11 **a** Dielectric constant studies for 25 wt% lithium acetate with 50 wt% PVA:50 wt% PVP polymer blend at different temperatures. **b** Dielectric loss studies for 25 wt% lithium acetate 50 wt% PVA:50 wt% PVP with polymer blend film at different temperatures. **c** DC conductivity dependence on dielectric constant (ε' at 1 MHz) for different temperatures of PVA/PVP with 25 wt% lithium acetate

The polarization current versus time for all the compositions of polymers is plotted as shown in Fig. 14, and ion transference number is tabulated in Table 5. From Table 5, transference number of polymer electrolytes is in the range of 0.94–0.82. It is confirmed that the charge transport in the investigated polymer electrolytes is predominately due to ions. The electron contribution is highly negligible in all the samples. The transference numbers (t_{ion}) of the present polymer electrolytes are close to unity [58, 59].

Bruce & Vincent method The Bruce–Vincent method is used to confirm the cationic and ionic transference number. The transference number corresponding to Li^+ ion transport is determined by means of Bruce–Vincent technique [60]. The result shows that the majority charge carriers are Li + ions. The values of the transference number are given in Table 5. In this technique, the electrochemical cell is made using the configuration: Silver electrode|MX (Electrolyte)|Silver electrode type. The cell is then characterized before and after polarization (after reaching the steady state) by means of electrochemical impedance spectroscopy (EIS) and corrects the formula by the factor pertaining to the alteration of cell parameters that can be easily obtained from the simple impedance spectrum. After polarization, initial (I_o)/final (I_s) currents are recorded.

$$t_{Li} = I_{ss}\left(V - I_0 R_0\right)/I_0\left(V - I_{ss}R_{ss}\right) \tag{9}$$

The ionic transference numbers calculated by Bruce–Vincent method are given in Table 5. The cole–cole plot for the higher-conductivity polymer electrolyte before and after polarization is given in Fig. 15. From this, we understand that the conductivity of the sample decreases after polarization.

Conclusion

50 wt% PVA:50 wt% PVP polymer blend with different weight concentrations of lithium acetate are prepared by solution casting method. In XRD analysis, the small hump appeared at $2\theta = 20°$ is broadened which indicates the increase in amorphous nature of the polymer blend by the inclusion of LiAce. The hump appeared at $2\theta = 31°$ and 40° is increased in broadness due to the inclusion of LiAce. By increasing the concentration of LiAce, the broadness of the hump decreased. This is mainly due to the short range order of LiAce. The shifting of transmittance bands in the FTIR analysis are obtained due to the interaction of hydrogen bonding between hydroxyl groups of PVA and carbonyl groups of PVP with the addition of LiAce. These results specified the miscibility of polymer. The DSC analysis of the polymer electrolyte shows that 25 wt% of lithium acetate-doped PVA/PVP system has lower glass transition temperature (0.67 eV). The

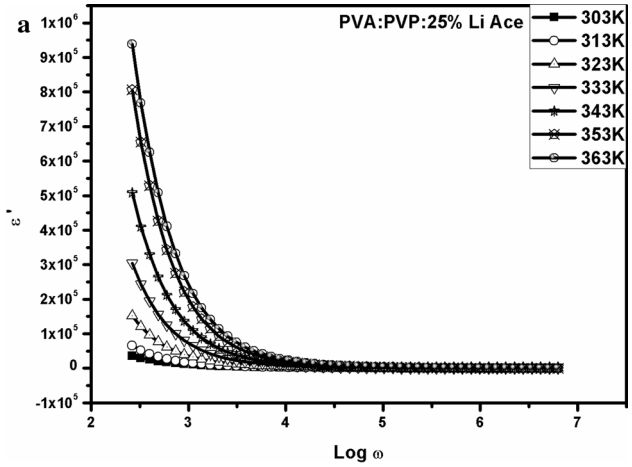
a
PVA:PVP:25% Li Ace
303K
313K
323K
333K
343K
353K
363K
ε '
Log ω

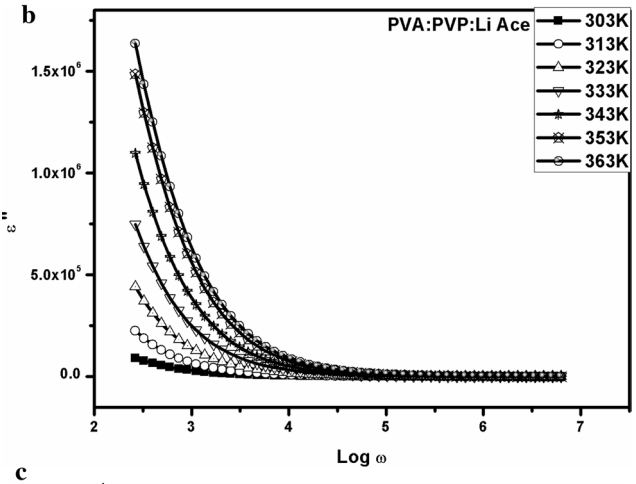
b
PVA:PVP:Li Ace
303K
313K
323K
333K
343K
353K
363K
ε "
Log ω

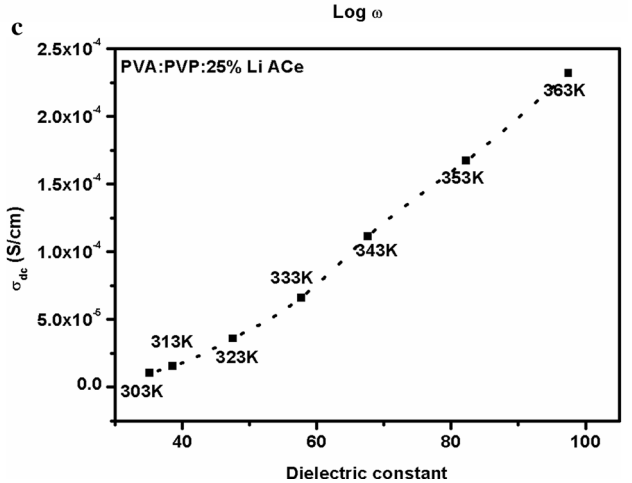
c
PVA:PVP:25% Li ACe
303K
313K
323K
333K
343K
353K
363K
σdc (S/cm)
Dielectric constant

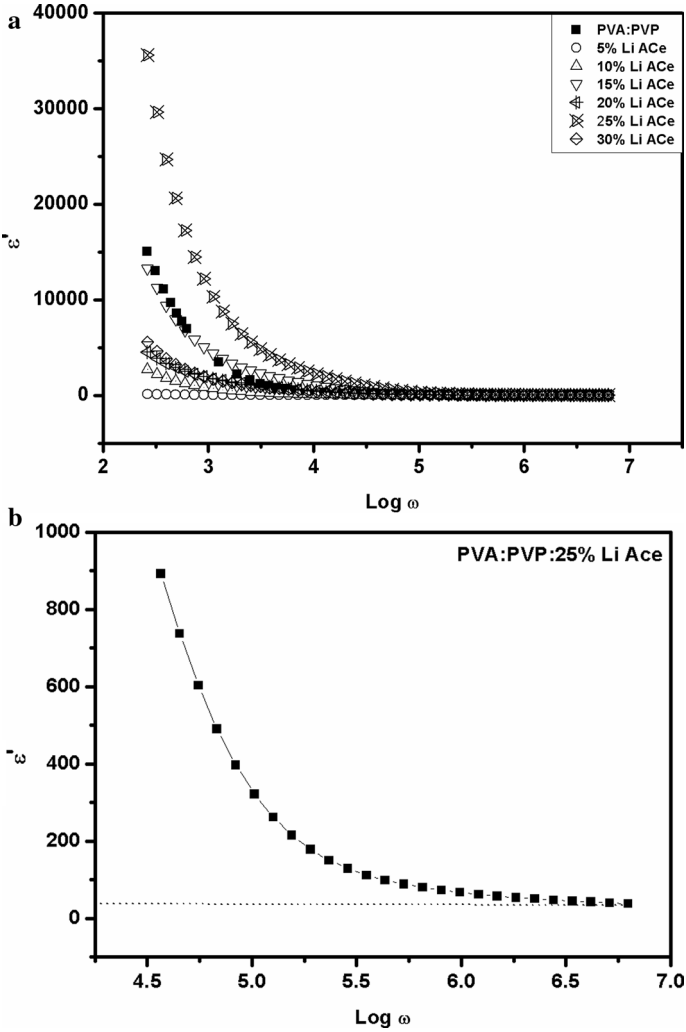

Fig. 12 **a** Dielectric constant for different compositions of lithium acetate. **b** Dielectric constant with frequency for 25 wt% lithium acetate mixed with PVA/PVP polymer matrix

SEM images show the dispersion of salt in the electrolytes and their smooth surface. The complex impedance plot indicates the increase in conductivity by the addition of LiAce with PVA/PVP. The PVA/PVP/lithium acetate(50:50:25) system gives the higher conductivity of 5.79×10^{-6} S cm^{-1} at 303 K and 1.40×10^{-4} S cm^{-1} at 363 K, respectively. The temperature dependence of the conductivity fits the Arrhenius and the VTF equations in different temperature ranges. The dielectric analysis and loss tangent

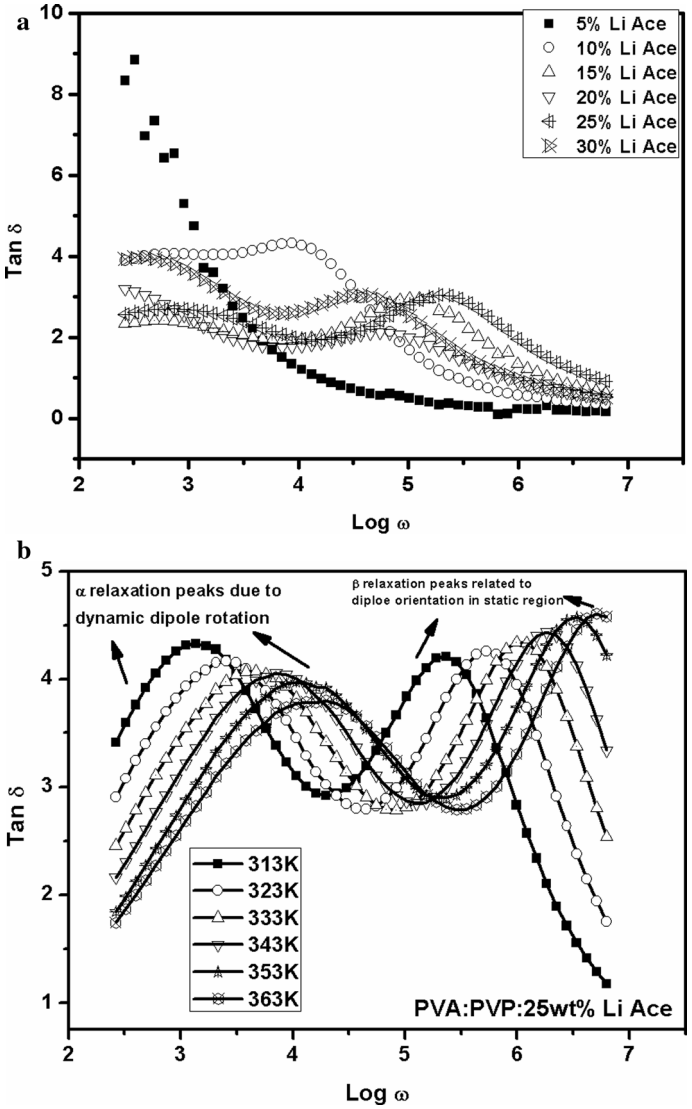

Fig. 13 **a** Loss tangent spectra of different wt% of lithium acetate-doped PVA/PVP polymer matrix. **b** Loss tangent spectra of 25 wt% lithium acetate-doped polymer system

analysis of the higher conducting polymer blend is also carried out at different temperatures. The dielectric constant increases due to the separation of ions and the vibration of the polymer chain segment and thereby increasing the conductivity. From loss tangent spectra, it is identified that low frequency α relaxation peaks are due to the dynamic

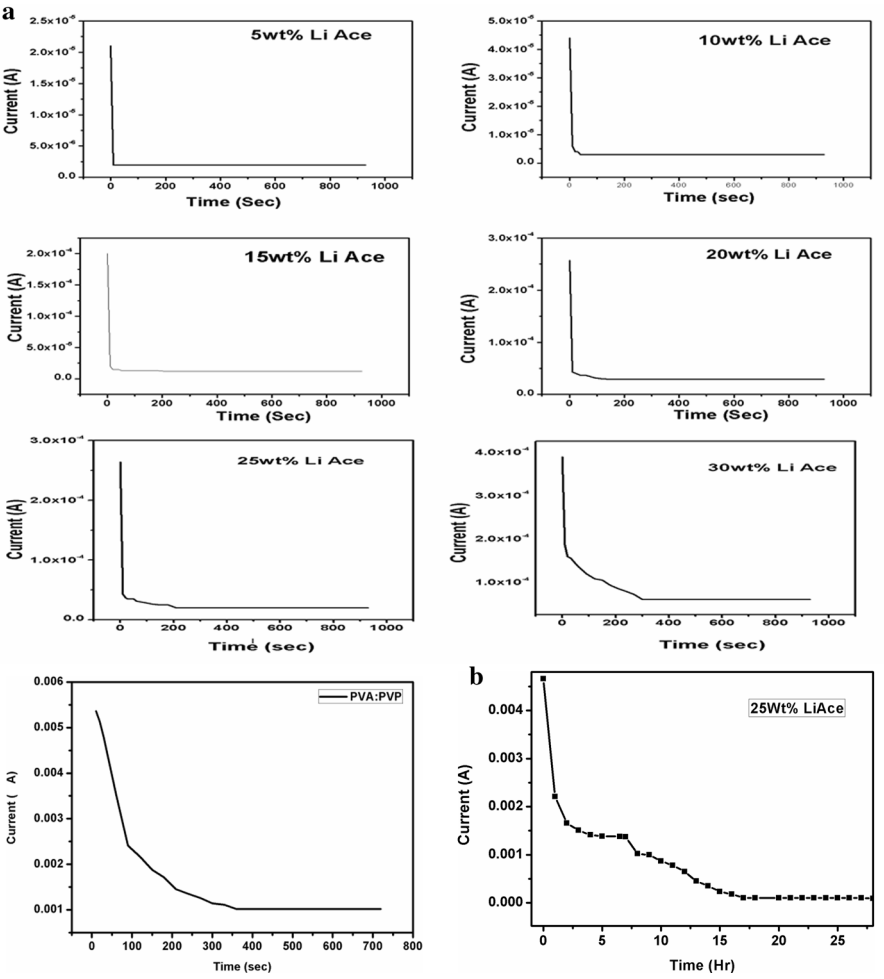

Fig. 14 **a** Transference number analysis of 50 wt% PVA:50 wt% PVP with different wt% lithium acetate using Wagner's polarization technique. **b** Transference number of 25 wt% lithium acetate blend with 50 wt% PVA:50 wt% PVP polymer using Bruce–Vincent method

dipole rotation and the high frequency β relaxation peaks are due to dipole orientation in static region. The high frequency peak related to amorphous phase is increased for higher-conductivity polymer electrolyte. These findings are clearly in agreement with the structural and impedance analysis. Transference number has been calculated from Wagner's polarizing technique and Bruce–Vincent method. From this, it is concluded

Table 5 Ionic transference number of PVA/PVP blends with different compositions of lithium acetate

Polymer systems	Transference number from Wagner's technique	Transference number from Bruce–Vincent method
50 wt% PVA/50 wt% PVP	0.82	0.81
50 wt% PVA/50 wt% PVP/5 wt% lithium acetate	0.90	0.83
50 wt% PVA/50 wt% PVP/10 wt% lithium acetate	0.91	0.85
50 wt% PVA/50 wt% PVP/15 wt% lithium acetate	0.94	0.82
50 wt% PVA/50 wt% PVP/20 wt% lithium acetate	0.90	0.82
50 wt% PVA/50 wt% PVP/25 wt% lithium acetate	0.92	0.86
50 wt% PVA/50 wt% PVP/30 wt% lithium acetate	0.85	0.81

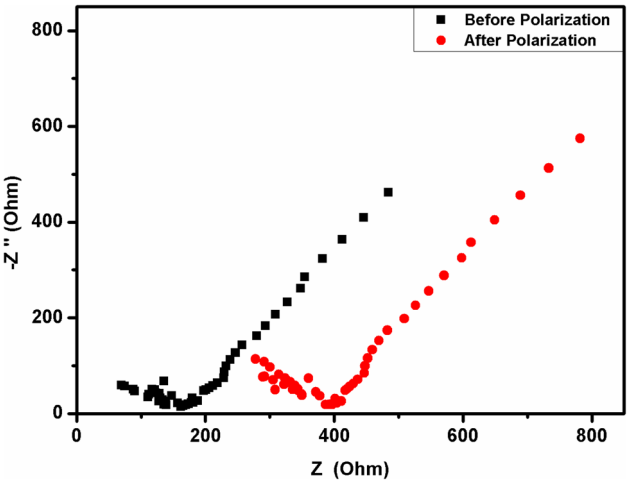

Fig. 15 Cole–cole plot before and after transference number analysis for maximum conductivity polymer electrolyte

that the conductivity of polymer electrolytes is due to ions only. So the prepared polymer electrolytes can be used in electrochemical cells.

Acknowledgements The authors thank the management of Kalasalingam Academy of Research and Education for Providing facilities and fellowships to carry out the research.

References

1. Hadi AG, Lafta F, Hashim A, Hakim H, Al-Zuheiry AIO, Salman SR, Ahmed H (2013) Study the effect of barium sulphate on optical properties of polyvinyl alcohol (PVA). Univers J Mater Sci 1:52–55

2. Hassan MA, Gouda ME, Sheha E (2010) Investigations on the electrical and structural properties of PVA doped with $(NH_4)_2SO_4$. J Appl Polym Sci 116:1213–1217
3. De-Queiroz AAA, Soares DAW, Trzesniak P, Gustavo A (2001) Abraham resistive-type humidity sensors based on PVP-Co and PVP-I_2 complexes. J Polym Sci 39:459–469
4. Gouda ME, Badr SK, Hassan MA, Sheha E (2011) Impact of ethylene carbonate on electrical properties of PVA/$(NH_4)_2SO_4$/H_2SO_4 proton-conductive membrane. Ionics 17:255–261
5. El-Khodary A (2010) Evolution of the optical, magnetic and morphological properties of PVA films filled with $CuSO_4$. Phys B 405:3401–3408
6. Sharaf F, Mansour SA, El-Lawindy AMY (1999) Mechanical and relaxation properties of γ-irradiated PVA doped with ferrous sulphate. Polym Degrad Stab 66:173–177
7. Basha AF, Basha MAF (2012) Structural and thermal degradation studies on thin films of the nanocomposite system PVP-Ce$(SO_4)_2 \cdot 4H_2O$. Polym Bull 68:151–165
8. Uma T, Mahalingam T, Stimming U (2004) Conductivity and thermal studies of solid polymer electrolytes prepared by blending polyvinylchloride, polymethylmethacrylate and lithium sulfate. Mater Chem Phys 85:131–136
9. Sandu T, Sarbu A, Damian CM, Patroi D, Iordache TV, Budinova T, Tsyntsarski B, FerhatYardim M, Sirkecioglu A (2015) Functionalized bicomponent polymer membranes as supports for covalent immobilization of enzymes. React Funct Polym 96:5–13
10. Caprarescu S, Miron AR, Purcar V, Radu AL, Sarbu A, Nicolae CA, (Neagu) Pascu M, Ion-Ebrasu D, Raditoiu V (2018) Treatment of Crystal violet from synthetic solution using membranes doped with natural fruit extract. CLEAN—Soil, Air, Water 46. Article number 1700413
11. Caprarescu S, Miron AR, Purcar V, Radu AL, Sarbu A, Ion-Ebrasu D, Atanase LI, Ghiurea M (2016) Efficient removal of Indigo Carmine dye by a separation process. Water Sci Technol 74:2462–2473
12. Ebrasu D, Stamatin I, Vaseashta A (2008) Proton-conducting polymers as electrolyte for fuel cells. NANO 3:381–386
13. Caprarescu S, Miron AR, Purcar V, Radu AL, Sarbu A, Ianchis R, Ion Erbasu D (2017) Commercial gooseberry buds extract containing membrane for removal of methylene blue dye from synthetic wastewaters. Rev Chim (Bucharest) 68:1757–1762
14. Yahya MZA, Arof AK (2003) Effect of oleic acid plasticizer on chitosan–lithium acetate solid polymer electrolytes. Eur Polymer J 39:897–902
15. Ismail L, Majid SR, Arof AK (2013) Conductivity study in PEO–LiOAc based polymer electrolyte. Mater Res Innov 13:282–284
16. Abdelrazek EM, Elashmawi IS, El-KhodaryA YassinA (2010) Structural optical thermal and electrical studies on PVA/PVP blends filled with lithium bromide. Curr Appl Phys 10:607–613
17. Su J, Ma ZY, Scheinbeim JI, Newman BA (1995) Ferroelectric and piezoelectric properties ofnylon 11/poly (vinylidene fluoride) bilaminate films. J Polym Sci Polym Phys 33:85–91
18. Tawansi A, Zidan HM (1990) Magnetic effects of the interfacial solitons in polystyrene composites. J Phys D Appl Phys 23:1320
19. KimSJ Park SJ, KimIY Lee YH, Kim SI (2002) Thermal characteristics of poly (VinylAlcohol) and poly (Vinylpyrrolidone) IPNs. J Appl Polym Sci 86:1844–1847
20. Yu H, Xu X, Chen X, Lu T, Zhang P, Jing X (2007) Preparation and antibacterial effects of PVA–PVP hydrogels containing silver nanoparticles. J Appl Polym Sci 103:125–133
21. Qiao J, Fu J, Lin R, Ma J, Liu J (2010) Alkaline solid polymer electrolyte membranes based on structurally modified PVA/PVP with improved alkali stability. J Polymer 51:4850–4859
22. Tripathi Mridula, Trivedi Shivangi, Dhar Ravindra, Singh Markandey, Pandey ND, Agrawal SL (2011) Structural and thermal studies of [PVA-LiAc]: TiO_2 polymer nanocomposite system. Phase Trans 84:972–980
23. Wen Z, Itoh T, Ichikawa Y, Kubo M, Yamamoto O (2000) Blend-based polymer electrolytes of poly (ethylene oxide) and hyper branched poly [bis(triethylene glycol)benzoate] with terminalacetyl groups. Solid State Ion 134:281–289
24. Bhajantri RF, Ravindrachary V, Poojary B, Ismayil Harisha A, Crasta V (2009) Studies on fluorescent PVA + PVP + MPDMAPP composite films. Polym Eng Sci 49:903–909
25. Basha MAF (2010) Magnetic and optical studies on polyvinylpyrrolidone thin films doped with rare earth metal salts. Polym J 42:728–734
26. Jaipal Reddy M, SreepathiRao S, Laxminarsaiah E, SubbaRao UV (1995) study of a thin film electrochemical cell based on (PVP + $AgNO_3$) electrolyte. Solid State Ion 80:93–98

27. Jaipal Reddy M, Sreekanth T, Chandrashekar M, Subbarao UV (2000) Ion transport and electrochemical cell characteristic studies of a new ($PVP + NaNO_3$) polymer electrolyte system. J Mater Sci 35:2841
28. Armand M (1983) Polymer solid electrolytes—an overview. Solid State Ionics 9–10:745–754
29. Zidan HM, Tawansi A, Abu-Elnader M (2003) Miscibility, optical and dielectric properties of UV-irradiated poly(vinylacetate)/poly(methylmethacrylate) blends. Phys B 339:78–86
30. SudhaKamath MK, Harish kumar HG, Chandramani R, Radhakrishna MC (2015) PVP influence on PVA crystallinity and optical band Gap. Arch Phys Res 6(2):18–21
31. Rajeswari N, Selvasekarapandian S, Karthikeyan S, Sanjeeviraja C, Iwai Y, Kawamura J (2013) Structural, vibrational, thermal, and electrical properties of PVA/PVP biodegradable polymer blend electrolyte with CH_3COONH_4. Ionics 19:1105
32. Shujahadeen BA, Mariwan AR, Ahang MH, Hameed MA (2017) Fabrication of polymer blend composites based on $[PVA\text{-}PVP]_{(1-x)}$: $(Ag_2S)_x$ $(0.01 \leq x \leq 0.03)$ with small optical band gaps: structural and optical properties. Mater Sci Semicond Process 71:197–203
33. Shujahadeen BA, Ranjdar MA (2018) Crystalline and amorphous phase identification from the tan δ relaxation peaks and impedance plots in polymer blend electrolytes based on [CS:AgNt]x:PEO(x–1) $(10 \leq x \leq 50)$. Electrochim Acta 285:30–46
34. Hodge RM, Edward GH, Simon GP (1996) Water absorption and states of water in semicrystalline poly (vinyl alcohol) films. Polymer 37:1371–1376
35. Rajeswari N, Selvasekarapandian S, MoniPrabu Karthikeyan S, Sanjeeviraja C (2013) Lithium ion conducting solid polymer blend electrolyte based on bio-degradable polymers. Bull Mater Sci 36:333–339
36. Abdelrazek EM, Elashmawi IS, El-khodary A, Yassin A (2010) Structural, optical, thermal and electrical studies on PVA/PVP blends filled with lithium bromide. Curr Appl Phys 2:607–613
37. Laot CM, Marand E, Oyama HT (1999) Spectroscopic characterization of molecular interdiffusion at a poly(vinyl pyrrolidone)/vinyl ester interface. Polym 40:1095
38. Wu H, Wu I, Chang F (2001) The interaction behavior of polymer electrolytes composed of poly(vinyl pyrrolidone) and lithium perchlorate (LiClO4). Polym. 42:555
39. Ravi M, Pavani Y, KiranKumar K, Bhavani S, Sharma AK, NarasimhaRao VVR (2011) Studies on electrical and dielectric properties of PVP: $KBrO_4$ complexed polymer electrolyte films. Mater Chem Phys 130:442–448
40. Malathi J, Kumaravadivel M, Brahmanandhan GM, Hema M, Baskaran R, Selvasekarapandian S (2010) Structural, thermal and electrical properties of PVA- $LiCF_3SO_3$ polymerelectrolyte. J Non-Cryst Solids 356:2277–2281
41. Shujahadeen BA (2016) Structural, morphological and electrochemical impedance study of CS:LiTf based solid polymer electrolyte: reformulated Arrhenius equation for ion transport study. Int J Electrochem Sci 11(11):9228–9244
42. Deshmukh K, Ahamed MB, Polu AR (2016) Impedance spectroscopy, ionic conductivity and dielectric studies of new Li + ion conducting polymer blend electrolytes based on biodegradable polymers for solid state battery applications. J Mater Sci Mater Electron 27:11410
43. Ambika C, Hirankumar G (2016) Characterization CH_3SO_3H-doped PMMA/PVP blend-based proton-conducting polymer electrolytes and its application in primary battery. J Appl Phys A Mater Sci Process 122:113
44. Shujahadeen BA, ZulHazrin ZA (2015) Ion-transport study in nanocomposite solid polymer electrolytes based on chitosan: electrical and dielectric analysis. J Appl Polym Sci 132:41774
45. Aziz SB (2013) Li^+ ion conduction mechanism in poly (ε-caprolactone)-based polymer electrolyte. Iran Polym J 22:877
46. Salleh NS, Shujahadeen BA, Aspanut Z, Kadir MFZ (2016) Electrical impedance and conduction mechanism analysis of biopolymer electrolytes based on methyl cellulose doped with ammonium iodide. Ionics 22:2157
47. Aziz SB (2018) The mixed contribution of ionic and electronic carriers to conductivity in chitosan based solid electrolytes mediated by CuNt Salt. J Inorg Organomet Polym 28:1942
48. Jonscher AK (1977) The 'universal' dielectric response. Nature 267:673–679
49. Shujahadeen BA (2016) Role of dielectric constant on ion transport: reformulated arrhenius equation. Adv Mater Sci Eng. https://doi.org/10.1155/2016/2527013
50. Shujahadeen BA, ZulHazrin ZA (2014) Electrical and morphological analysis of chitosan: AgTf solid electrolyte. Mater Chem Phys 144:280–286

51. Shujahadeen BA, Thompson JW, Mohd FZK, Hameed MA (2018) A conceptual review on polymer electrolytes and ion transport models. J Sci Adv Mater Dev 3:1–17
52. Ahamad MN, Varma KBR (2010) Dielectric properties of (100-x) Li2B4O7 x(Ba5Li2Ti2Nb8O30) glasses and glass nanocrystal composites. Mater Sci Eng B 167:193–201
53. Mohd Z, Iqbal Rafiuddin (2016) Structural electrical conductivity and dielectric behavior of Na_2SO_4–LDT composite solid electrolyte. J Adv Res 7:135–141
54. Dieterich W, Maass P (2002) Non-Debye relaxations in disordered ionic solids. Chem Phys 284:439–467
55. Shujahadeen BA, Ranjdar MA, Mariwan AR, Hameed MA (2017) Role of ion dissociation on DC Conductivity and silver nanoparticle formation in PVA:AgNt based polymer electrolytes: deep Insights to Ion transport mechanism. Polymers 9(8):338
56. Shujahadeen BA, Faraj MG, Omed G. Abdullah (2018) Impedance Spectroscopy as a Novel Approach to Probe the Phase Transition and Microstructures Existing in CS:PEO Based Blend Electrolytes 8:1430
57. Joncher AK (1987) Analysis of the alternating current properties of ionic conductors. Matter Sci 13:553–562
58. Bhargav PB, Mohan VM, Sharma AK, Rao VVRN (2009) Investigations on electrical properties of (PVA:NaF) polymer electrolytes for electrochemical cell applications. Curr Appl Phys 9:165–171
59. Funke K, Roling B, Lange M (1998) Dynamics of mobile ions in crystals, glasses and Melts. Solid State Ion 105:195–208
60. Vanitha D, Asathbahadur S, Nallamuthu N, Athimoolam S (2018) Structural, thermal and electrical properties of polyvinyl alcohol/poly(vinyl pyrrolidone)–sodium nitrate solid polymer blend electrolyte. Ionics 24:139–151